

## Optimization Design of NACA 4412 Airfoil Based on Genetic Algorithm for Efficiency and Maximum Lift Force

Aryo Eko Laksono<sup>1\*</sup>, Aldias Bahatmaka<sup>1</sup>, Deni Fajar Fitriyana<sup>1</sup>, Galih TriLaksono<sup>1</sup>, Muhammad Habibullah<sup>1</sup>,  
Haris Nubli<sup>2</sup>, Cho Joung Hyung<sup>3</sup>

<sup>1</sup>Department of Mechanical Engineering, Faculty of Engineering, Semarang State University, Sekaran Campus,  
Gunungpati, Semarang 50229, Central Java, Indonesia

<sup>2</sup>Department of Fluid Mechanics, Gas Explosion, Fire Risk Analysis, Structural Mechanics, School of Engineering,  
University of Surrey, United Kingdom

<sup>3</sup>Interdisciplinary Program of Marine Design Convergence, Pukyong National University, Busan 48513, South Korea  
\*E-mail: aryoekolaksono1928@students.unnes.ac.id,

Submitted: 16-06-2025; Accepted: 11-08-2025; Published: 31-08-2025

### Abstract

The NACA 4412 airfoil, renowned for its exceptional subsonic aerodynamic performance, faces critical operational constraints including elevated drag characteristics and premature stall onset at high angles of attack. While previous investigations have independently examined internal slot modifications and gurney flap implementations for aerodynamic enhancement, the synergistic potential of their combined application to the NACA 4412 configuration remains largely unexplored. This research presents a comprehensive optimization study that strategically integrates internal slot geometry with gurney flap configuration to maximize lift coefficient (CL) and aerodynamic efficiency (CL/CD) through advanced genetic algorithm optimization. The methodology employed high-fidelity computational fluid dynamics simulations (CFD) using FLUENT with Spalart-Allmaras turbulence modeling, validated against experimental data to ensure accuracy. PCHIP numerical interpolation techniques were utilized to estimate aerodynamic coefficients across comprehensive angle-of-attack ranges not directly simulated. The optimized configuration demonstrated remarkable performance improvements, including a 75.68% increase in lift coefficient, an extension of the critical stall angle from 14° to 16°, enhanced aerodynamic efficiency, and significantly improved flow stability with reduced separation characteristics. These findings establish that the synergistic combination of internal slot and gurney flap modifications can fundamentally transform NACA 4412 aerodynamic performance, particularly excelling in high-angle-of-attack operational scenarios.

**Keywords:** airfoil; genetic algorithm; gurney flap; internal slot

### Abstrak

Profil sayap NACA 4412, yang terkenal karena kinerja aerodinamis subsoniknya yang luar biasa, menghadapi batasan operasional kritis termasuk karakteristik drag yang tinggi dan terjadinya stall dini pada sudut serang tinggi. Meskipun penelitian sebelumnya telah secara terpisah mengkaji modifikasi slot internal dan implementasi flap gurney untuk peningkatan aerodinamis, potensi sinergis dari penerapan gabungan keduanya pada konfigurasi NACA 4412 masih belum banyak dieksplorasi. Penelitian ini menyajikan studi optimasi komprehensif yang secara strategis mengintegrasikan geometri slot internal dengan konfigurasi flap gurney untuk memaksimalkan koefisien angkat (CL) dan efisiensi aerodinamis (CL/CD) melalui optimasi algoritma genetika canggih. Metode yang digunakan melibatkan simulasi dinamika fluida komputasional (CFD) berpresisi tinggi menggunakan FLUENT dengan model turbulensi Spalart-Allmaras, yang diverifikasi dengan data eksperimental untuk memastikan akurasi. Teknik interpolasi numerik PCHIP digunakan untuk memperkirakan koefisien aerodinamika pada rentang sudut serang yang luas yang tidak disimulasikan secara langsung. Konfigurasi yang dioptimalkan menunjukkan peningkatan kinerja yang signifikan, termasuk peningkatan koefisien angkat sebesar 75,68%, perpanjangan sudut stall kritis dari 14° menjadi 16°, efisiensi aerodinamika yang lebih baik, dan stabilitas aliran yang jauh lebih baik dengan karakteristik pemisahan yang berkurang. Temuan ini menunjukkan bahwa kombinasi sinergis antara modifikasi slot internal dan flap gurney dapat secara fundamental mengubah kinerja aerodinamika NACA 4412, terutama unggul dalam skenario operasional sudut serang tinggi.

**Kata kunci:** airfoil; algoritma genetika; gurney flap; slot internal

### 1. Introduction

NACA 4412 is a profile widely used in subsonic aerodynamic systems, especially at low to medium speeds, such as in wind turbines and light aircraft [1]. The main advantage of this aerodynamic profile is its ability to generate a high lift

coefficient at medium to high angles of attack and a relatively stable pressure distribution under subsonic flow conditions [2]. The main advantage of this aerodynamic profile is its ability to generate a high lift coefficient at medium to high angles of attack, as well as a relatively stable pressure distribution under subsonic flow conditions [3]. Meanwhile, a Gurney flap at a 2% chord height on the Eppler 423 airfoil was reported to significantly increase aerodynamic efficiency, with lift remaining high up to  $14^\circ$  AoA. The mechanism of this enhancement is due to the increased effective camber and more stable pressure distribution on the Airfoil profile's pressure surface [4].

Recent research has demonstrated significant potential for improving NACA 4412 airfoil performance through geometric modifications. Internal slots can create pathways for high-momentum fluid flow from the pressure surface to the suction surface, effectively preventing flow separation and enhancing aerodynamic performance [6]. Research by Rayhan et al. found that NACA 4412 airfoils with internal slots achieve approximately 35% higher lift coefficients than standard configurations at high angles of attack, with stall angles improved from  $14^\circ$  to  $17^\circ$  [1]. Furthermore, combining slots with groove modifications can extend stall angles by up to  $18^\circ$ , providing enhanced performance characteristics for applications that require operation at higher angles of attack [1]. The effectiveness of slot modifications is attributed to their ability to delay boundary layer separation by energizing it with high-momentum flow, which is especially beneficial at higher angles of attack where early stall is common [4][1]. Groove modifications further delay separation, reducing drag forces and improving overall aerodynamic efficiency [1]. While these improvements have been tested on various aerodynamic profiles, their application is typically studied in isolation either slot, groove, or Gurney flap and rarely in combination on the NACA 4412.

While internal slots and Gurney flaps have proven effective for airfoil enhancement, existing research predominantly examines these modifications independently rather than synergistically. Comprehensive studies investigating the combined implementation of these methods on NACA 4412 profiles remain limited. This research evaluates the integrated aerodynamic effects of dual modification strategies on NACA 4412 performance. The investigation employs Computational Fluid Dynamics (CFD) to analyze lift coefficient (CL), drag coefficient (CD), and aerodynamic efficiency (CL/CD). Multi-parameter optimization through Genetic Algorithm implementation in MATLAB identifies optimal geometric configurations [5]. The study focuses on geometric variations and flow characteristics, excluding material and structural considerations. This research makes three primary contributions: a quantitative assessment of the combined slot-flap effects on NACA 4412 aerodynamics; the development of a multi-parameter optimization framework using genetic algorithms; and the establishment of an integrated methodology that combines PCHIP interpolation with CFD simulations for precise performance prediction.

## 2. Material and Method

This study evaluates the aerodynamic performance of the NACA 4412 airfoil under various flow conditions using the CFD method. Since experimental approaches have high risks and costs, a numerical approach is appropriate for investigating the problem [6]. To achieve this goal, CFD simulations were performed to examine the lift and drag characteristics of the airfoil. The results of these simulations are then validated with experimental data from previous studies [1].

### 2.1 Governing Equations

The calculation of fluid flow around the airfoil profile is performed using a numerical method based on the steady-state solution of the RANS equations, as shown in Equations (1) and (2). The continuity equation describes mass conservation, while the momentum equation describes fluid momentum conservation in the X-axis direction [7].

$$\frac{\partial \rho}{\partial t} + \frac{\partial}{\partial x_i} (\rho u_i) = 0 \quad (1)$$

$$\frac{\partial \rho}{\partial t} (\rho u_i) + \frac{\partial}{\partial x_i} (\rho u_i u_j) = \frac{\partial}{\partial x_i} + \frac{\partial}{\partial x_i} \left[ \mu \left( \frac{\partial u_i}{\partial x_i} + \frac{\partial u_i}{\partial x_i} - \frac{2}{3} \delta_{ij} \frac{\partial u_i}{\partial x_i} \right) \right] + \frac{\partial}{\partial x_i} (-\rho x_i' u_i') = 0 \quad (2)$$

The turbulence model used in this study is the Spalart-Allmaras model, which is known for its high numerical stability and good accuracy in aerodynamic flows with medium to high Reynolds numbers [8]. The transport equation for the work variable  $\tilde{v}$  is presented in Equation (3).

$$\frac{\partial}{\partial t} (\rho \tilde{v}) + \frac{\partial}{\partial x_i} (\rho \tilde{v} u_i) = G_v + \frac{1}{\sigma_{\tilde{v}}} \left[ \frac{\partial}{\partial x_j} \left\{ (\mu + \tilde{v} \frac{\partial \tilde{v}}{\partial x_j}) \right\} + C_{b2\rho} \left( \frac{\partial \tilde{v}}{\partial x_j} \right)^2 \right] - Y_v + S_{\tilde{v}} \quad (3)$$

## 2.2 Geometry

In this study, the NACA 4412 airfoil profile is investigated by analyzing twelve geometric configurations: baseline and the modified design obtained through an optimization process using a genetic algorithm. Gurney flaps and internal slots are passive flow control devices that optimize the aerodynamic performance of airfoils through different but complementary mechanisms. The Gurney flap, positioned perpendicular to the trailing edge, works by creating a complex vortex system that generates a low-pressure zone and increases the virtual camber of the airfoil. Research by Karthikeyan and Harish shows that flaps with heights of 1%, 2%, and 3% chord length can increase the lift coefficient by 35%, 58%, and 82%, respectively, through the formation of stable counter-clockwise primary vortices and secondary vortices in the near-wake region [9]. Meanwhile, internal slots function as a boundary layer control mechanism that utilizes natural pressure differences to transfer high-momentum fluid from the pressure surface to the suction surface, as demonstrated by the research of Ni et al [3].

Demonstrated that an optimal design with a width of 0.1c and a radius of 0.4c at the 40% chord position achieves a maximum lift coefficient increase of 58% and a lift-to-drag ratio of 14% through flow separation prevention and the creation of a virtual leading edge downstream. Both technologies exhibit distinct angle-of-attack-dependent characteristics, where the Gurney flap provides consistent lift enhancement with proportional drag penalties 32%, 57%, 83% for 1%, 2%, 3% lift, while internal slots experience initial loss at low AoA  $0^\circ < \text{AoA} < 11^\circ$  but are highly effective at moderate to high angles. Optimizing the performance of both devices depends on critical geometric parameters, such as the optimal height-to-chord ratio of 1–3% for the gurney flap and positioning the slots at the location of maximum differential pressure. This approach also allows for the potential integration of active systems to address the operational limitations of each technology **Figure 1**.



(a)



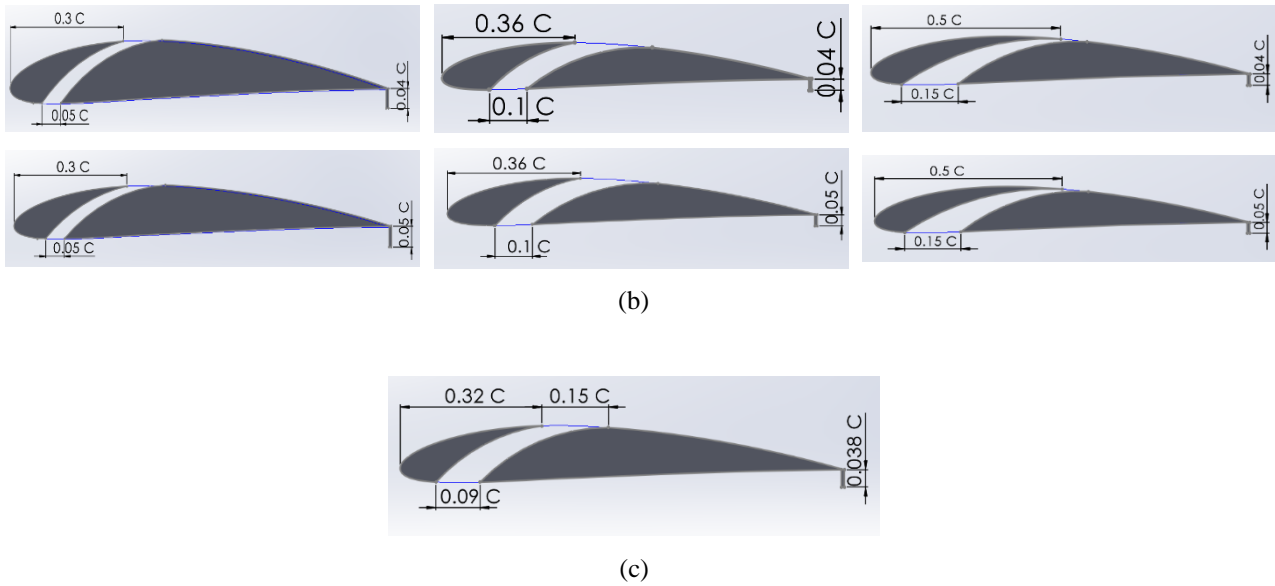


**Figure 1.** Airfoil NACA 4412, (a) Original NACA 4412 (b) 9 different internal slots and gurney flap (c) Optimization NACA 4412

### 2.3 Boundary Conditions

Boundary conditions are zones that serve as constraints in the fluid system so that the simulation can have conditions identical to real-world experiments [10]. The domain of this research has two boundary conditions, with the centre of the domain circle located at  $1/5$  of the leading edge of the airfoil [1]. A velocity inlet with a speed variation of 20 m/s is the first part of the domain. The number of reynolds used in this study is  $1.92 \times 10^5$ . The second part of the boundary condition is the outlet pressure with a value of 0 Pa. Then, the airfoil boundary condition is considered a wall with a no-slip condition. **Figure 2** illustrates the detailed dimensions of the boundary condition.

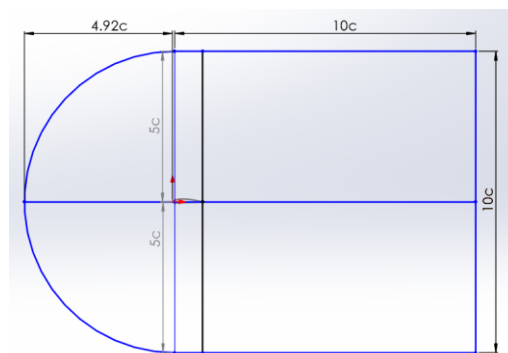


**Figure 2.** Boundary Conditions

### 2.4 Meshing

The meshing process is a method for dividing the simulation domain into smaller elements. This process is intended to improve the accuracy of the simulation [7]. On **Figure 3** the mesh used in this study is a quadrilateral mesh with an inflation layer around the airfoil wall to capture the boundary layer effect [11]. Mesh independence testing is conducted to ensure that the mesh size does not affect the simulation results. A structured type-C mesh improves the accuracy of modelling the boundary layer. Around the airfoil surface, the  $y^+$  value is kept below one so that recommendations for high-precision turbulence modelling can accurately simulate the viscous sublayer [12].

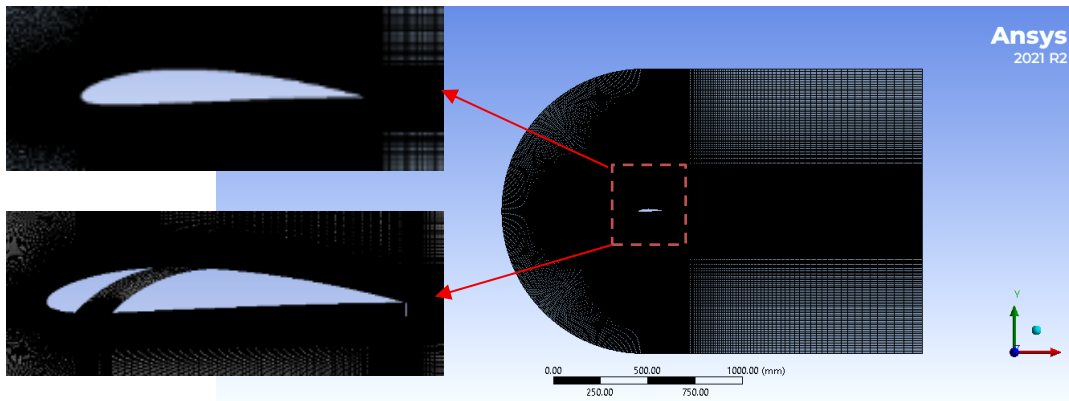


**Figure 3.** Mesh Baseline and Optimization

## 2.5 Aerodynamic of Airfoil

The aerodynamics of an airfoil is a field that relates to two main forces: lift and drag. Drag is the aerodynamic force that acts in the same direction as the fluid flow. At the same time, lift is defined as the force perpendicular to the direction of fluid flow [13]. Both of these forces are typically expressed in terms of dimensionless coefficients. The lift coefficient is a quantitative metric that measures the magnitude of the lift force. The drag coefficient is a quantitative measure of the magnitude of the drag force [14]. The calculation of these forces can be seen through the formulas in Equations (4), (5), and (6) below:

$$CL = \frac{2D}{\rho u^2 c} \quad (4)$$

$$CD = \frac{2L}{\rho u^2 c} \quad (5)$$

$$\frac{CL}{CD} = \frac{CL}{CD} \quad (6)$$

## 2.6 Airfoil Design

The initial design issues of the NACA 4412 aircraft are explained in detail based on technical aerodynamic principles. The dependent variables, which include metrics such as chord length, air density, dynamic viscosity, and flow velocity, are shown in **Table 1**. Meanwhile, the independent variables affecting the internal slot position, the internal width of the lower slot, and the height of the gurney flap were analyzed and optimized in **Table 2**.

**Table 1.** Dependent variables.

Item	Unit
Series	NACA 4412
Chord	150 mm
Density	1.225 kg/m <sup>3</sup>
Viscosity	1,184 x 10 <sup>-5</sup> kg/m-s
Velocity	20 m/s

**Table 2.** Independent variables.

Category	I	II	III	IV	V	VI	VII	VIII	IX
Xslotup	0.3c	0.3c	0.3c	0.36c	0.36c	0.36c	0.5c	0.5c	0.5c
Xslotlo	0.05c	0.05c	0.05c	0.1c	0.1c	0.1c	0.15c	0.15c	0.15c
GF	0.03c	0.04c	0.05c	0.03c	0.04c	0.05c	0.03c	0.04c	0.05c

## 2.7 PCHIP Interpolation Method and Genetic Algorithm

This investigation employs numerical interpolation and genetic algorithm optimization to enhance NACA 4412 aerodynamic performance through integrated internal slot and Gurney flap modifications [15]. Lift and drag coefficients were determined via two-dimensional CFD simulations using Fluent software at attack angles of  $0^\circ$ ,  $16^\circ$ , and  $22^\circ$ . PCHIP (Piecewise Cubic Hermite Interpolating Polynomial) is a special interpolation method that facilitates the calculation of values between known data points [16]. This method is based on creating cubic functions at each data interval, resulting in a smooth curve [17]. Interpolation of the values of CL and CD at unavailable angles of attack ( $\alpha$ ) is achieved through the use of equations (7) and (8).

Genetic algorithms are search techniques inspired by natural selection and genetics principles. The algorithm searches for better solutions by randomly selecting the best solutions and combining them, similar to how humans search for solutions [18]. This approach provides enhanced effectiveness compared to conventional computational methods and traditional [5]. Three independent design variables were established using MATLAB: slot position  $x_1$ , slot width  $x_2$ , and gurney flap height  $x_3$  in Equation (14) to (16). Geometric constraints ensured aerodynamically optimal positioning while preventing excessive in Equation (17).

The fitness function maximizes aerodynamic efficiency through lift-to-drag ratio optimization (9) to (11). This instrument has two additional functions: penalty and bonus [19]. Incorporating a penalty function  $P(x_1, x_2)$  to prevent excessive slot elongation in Equation (12) and a bonus function  $B(x_1)$  for optimal Gurney flap configuration (13). The design parameter constraints used in the optimization process are determined through a comprehensive review of previous research and a rigorous examination of geometric constraints. The specific equations governing these boundaries are outlined in the following section. Final aerodynamic evaluation calculates lift, drag, and L/D efficiency using equations (18) to (20).

Interpolated

$$C_L \alpha = PCHIP(\alpha_{data}, C_{L,Data}, \alpha) \quad (7)$$

$$C_D \alpha = PCHIP(\alpha_{data}, C_{D,Data}, \alpha) \quad (8)$$

Fitness Fuction

$$\frac{\max}{x \in R^3} f(x) = \frac{\max}{x \in R^3} (C_L(x_1, x_2, x_3, \alpha) \cdot P(x) \cdot B(x)) \quad (9)$$

$$\frac{\max}{x \in R^3} f(x) = \frac{\max}{x \in R^3} (C_D(x_1, x_2, x_3, \alpha) \cdot P(x) \cdot B(x)) \quad (10)$$

$$\frac{\max}{x \in R^3} f(x) = \frac{\max}{x \in R^3} \left( \frac{C_L(x_1, x_2, x_3, \alpha)}{C_D(x_1, x_2, x_3, \alpha)} \cdot P(x) \cdot B(x) \right) \quad (11)$$

Where the design variables of the upper slot position ( $x_1$ ), lower slot width ( $x_2$ ), and gurney flap height ( $x_3$ ) are examined. CL, CD and CL/CD ratio, are obtained from CFD data that has been interpolated at a fixed angle of attack  $\alpha =$

16°. Functions  $f(x)$  and  $B(x)$  represent penalty (12) and bonus (13), functions integrated within the fitness function to maintain design constraints and optimize aerodynamic performance.

Penalty

$$f(x) = \{0.8 \text{ if } X_{slotup} + X_{slotlo} > 0.9 \text{ } 1.0 \text{ other} \quad (12)$$

Bonuses

$$B(x) = \{1.05 \text{ if } H_{GF} = 0.04 \text{ dan } \alpha \geq 15^\circ \text{ } 1.0 \text{ other} \quad (13)$$

Constrain

$$0.3c \leq x_1 \leq 0.5c \quad (14)$$

$$0.05c \leq x_2 \leq 0.15c \quad (15)$$

$$0.03c \leq x_3 \leq 0.05c \quad (16)$$

$$x_1 + x_2 \leq 0.9 \quad (17)$$

Calculation of aerodynamic forces:

$$L = C_L \cdot \frac{1}{2} \rho V^2 \cdot A \quad (18)$$

$$D = C_D \cdot \frac{1}{2} \rho V^2 \cdot A \quad (19)$$

$$\frac{L}{D} = \frac{C_L}{C_D} \quad (20)$$

In this study, the Genetic Algorithm (GA) was employed to ascertain the optimum aerodynamic performance of the initial airfoil configuration. The parameters and configuration for the Generalised Additive model GA used in this optimisation process are delineated in **Table 3**.

**Table 3.** Setting up the GA parameters.

Population size = 30	
Number of generations	100
Selection	Stochastic uniform
Crossover rate	0.8
Crossover function	Scattered
Mutation rate	feasibility

### 3. Result and Discussion

#### 3.1. Grid independence

To ensure the accuracy of numerical analysis, it is crucial to optimize network design, which is generally evaluated through network independence tests. The grid's shape, quality, and quantity are the primary considerations in designing an effective grid [20]. An independent grid study was conducted on the NACA 4412 Airfoil with an AoA of 10°. The results of CL, CD, and the CL/CD ratio are shown in **Table 4** Meshing with 346,500 and 410,500 elements show almost the same results, with CL error around 1.3% and CD 3–4%, indicating that convergence has been achieved. On the other hand, the mesh with 79,537 elements produced significant inaccuracies CL 12.39% and CD 26.10%. Therefore, a mesh of approximately 346,500–410,500 elements is optimal because it is very accurate and computationally efficient [1].

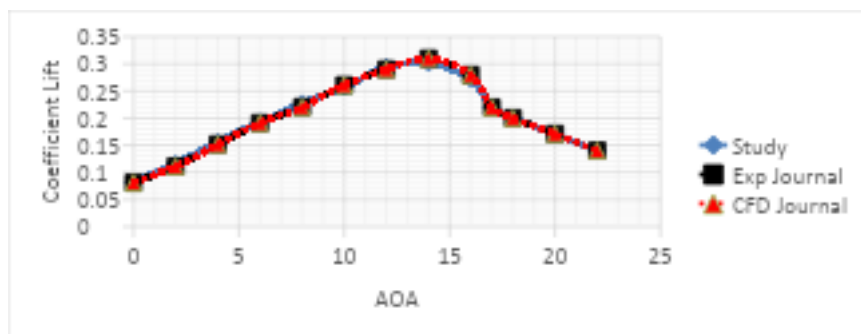
**Table 4.** Grid Independence

Element	CL	CD	CL/CD	CL Error	CD Error
410500	0.2574211	0.00675	38.16459	1.32%	3.64%
346500	0.2573115	0.00677	38.02712	1.36%	3.32%
201500	0.2789323	0.00739	37.76186	6.49%	5.36%
199000	0.256851	0.00681	37.72907	1.54%	2.69%
150500	0.2561319	0.00687	37.28531	1.83%	1.77%
104500	0.250324	0.00742	33.75391	4.19%	5.73%
79537	0.2320738	0.00946	24.53149	12.39%	26.10%

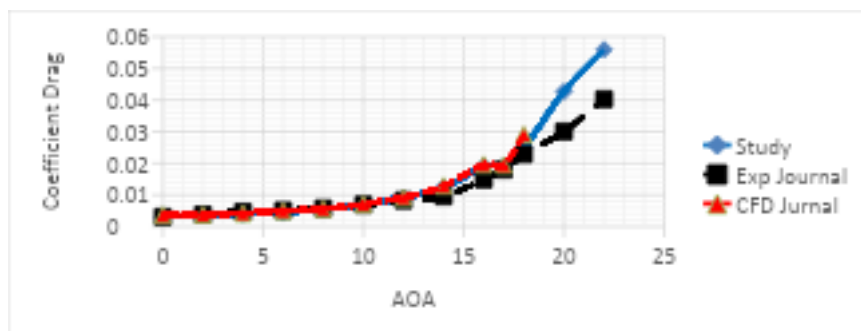
### 3.2. Validation of Original NACA 4412

The CFD simulation results align with the experimental data, validating this method for airfoil design optimization verification. Validation of the NACA 4412 airfoil was performed using CFD, and the results were compared to experimental data from Rayhan [1]. **Figure 4** compares the lift coefficient against the AoA, and the three curves exhibit the same trend, reaching maximum lift at AoA  $14^\circ$ . At an AoA of  $14^\circ$ , the differences become significant due to the complexities of turbulent flow, which are challenging to model accurately. The average error CL across all AoA is 1.67%. **Figure 6b** shows the drag force curve that follows a similar pattern between CFD and experiments. The difference in drag at AoA  $18^\circ$  is minor, but it becomes more significant at higher AoA.

The figure compares drag against angle of attack between study results, experimental data, and CFD from the journal. Each curve generally shows a similar trend: the drag force increases until it peaks at an AoA of  $8^\circ$ – $22^\circ$ . The study's findings indicate that the model is valid and consistent with CFD journal data. There are some differences with the experimental data, especially at low AoA, which the effects of testing conditions and turbulence models may cause. Based on this comparison, it can be concluded that the simulation can accurately depict aerodynamic characteristics, with the highest efficiency point CL/CD occurring before the onset of drag.

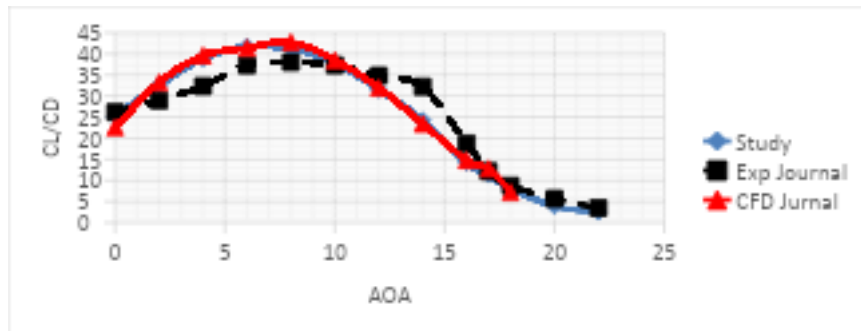


(a)



(b)





(c)

**Figure 4.** Validation Graph (a) Lift Coefficient (b) Drag Coefficient (c) CL/CD Ratio

### 3.3. Optimization Output

The optimum lift and aerodynamic efficiency output is presented in **Table 5**. **Figure 5** illustrates the results obtained from Genetic Algorithm optimization.

**Table 5.** Output

Iteration	Xslotup	Xslotlo	GF
51	0.31c	0.11c	0.038c

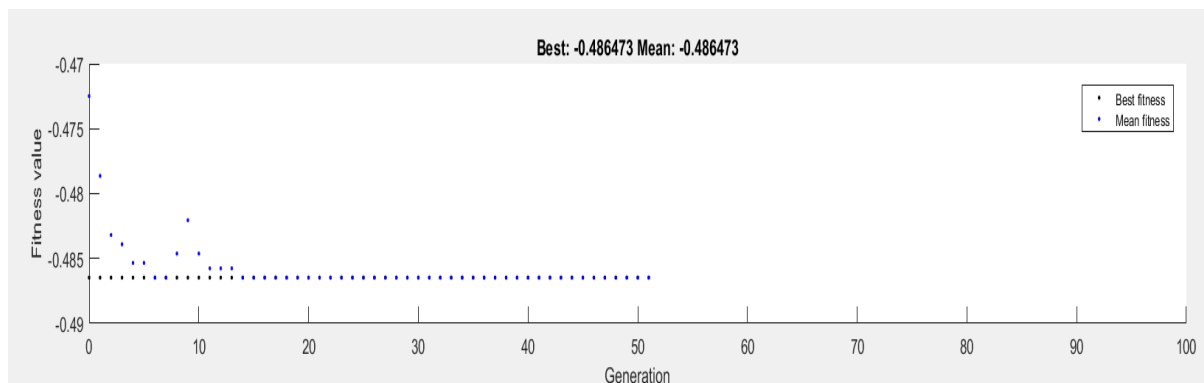


**Figure 5.** Fitness value through the generations

In the 51st iteration of the experiment, the lift and aerodynamic efficiency reach their optimal values when the slot width is 0.11c, the slot position is 0.31c, and the Gurney flap height is 0.038c of the chord length.

### 3.4. Final Result

The output of the optimal lift force can be shown in the **Table 6** and the results are exported using a genetic algorithm.

**Table 6.** Comparison of the optimized results

Result	Original	New	Improvements
CL	0.0074	0.013	75.68%

The simulation results are shown in **Figure 6**, Simulation results indicate that the airfoil with optimized geometry achieves significant aerodynamic improvements over the baseline design, with a 75.68% increase in lift coefficient across the angle of attack range and a stall delay of 2 ° from 14° to 16° AoA. The optimization's ability to enhance lift and extend the operational envelope by delaying flow separation is not without a downside, as it results in a 7.67% increase in drag

at  $16^\circ$  AoA, which must be considered when deciding on an aerodynamic compromise between lift enhancement and drag penalty.

Optimization has introduced some geometrical changes that appear to have fundamentally altered the behavior of the pressure distribution and boundary layer around the surface of an airfoil. Higher lift performance implies improved flow attachment features, especially at high angles of attack, making it particularly useful in applications that require maneuverability or operation in challenging flight conditions. The stall delay mechanism's geometry optimization leads to a more gradual flow separation. Nevertheless, the rise in drag is due to the underlying physics of lift generation, which implies that higher circulation and pressure differentials lead to greater viscous losses and high-pressure drag components.

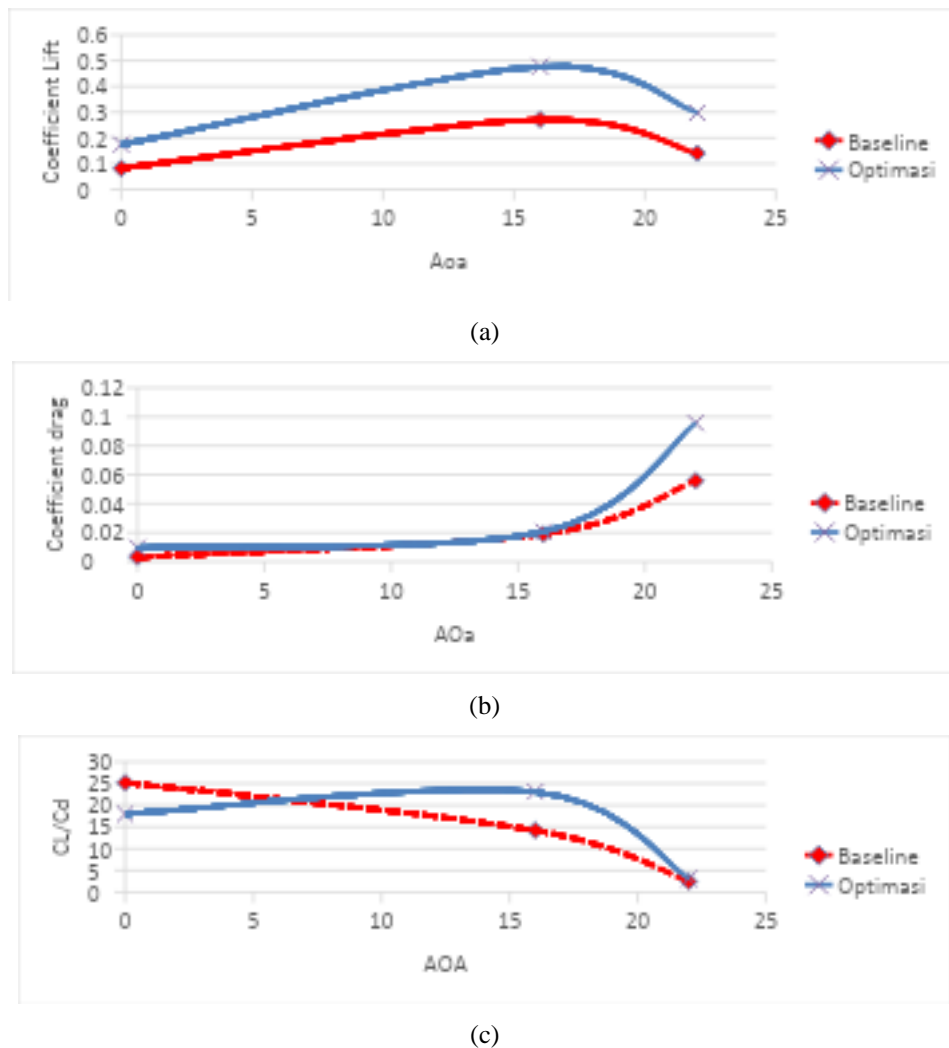


**Figure 6.** Optimization Graph, (a) Lift Coefficient (b) Drag Coefficient (c) CL/CD Ratio

In **Figure 7** the pressure distribution on the baseline NACA 4412 airfoil demonstrates more stable flow conditions with optimal aerodynamic efficiency characterized by high CL/CD ratio and smoother, more uniform pressure gradients, where under normal operating conditions, the baseline configuration exhibits conventional pressure characteristics with moderate pressure differential between upper and lower surfaces generating standard lift according to the NACA 4412 design specifications. However, when the angle of attack is increased to  $16^\circ$ , the baseline airfoil experiences significant performance degradation due to early flow separation and the formation of a wide wake, indicating reduced aerodynamic efficiency and a potential for stall occurrence at high angles of attack.

Conversely, the pressure distribution on the modified airfoil with internal slot and gurney flap at  $16^\circ$  angle of attack shows significant differences between upper and lower surfaces, with maximum pressure occurring on the lower surface resulting in lift generation consistent with Bernoulli's principle, where the internal slot functions to strengthen the boundary layer so that flow remains attached to the trailing edge [21]. In contrast, the gurney flap plays a role in increasing effective camber and lift coefficient through the formation of reverse flow vortices. Results of the airfoil configuration with internal slot and gurney flap at  $16^\circ$  AoA demonstrate significant CL increase and delayed stall compared to the standard airfoil configuration, indicating substantial performance improvement under high-lift conditions with the capability to maintain attached flow at high angles of attack where the baseline configuration already experiences significant performance degradation, thereby establishing the Outstanding aerodynamic characteristics of the modified design through enhanced pressure differential management and boundary layer control mechanisms.

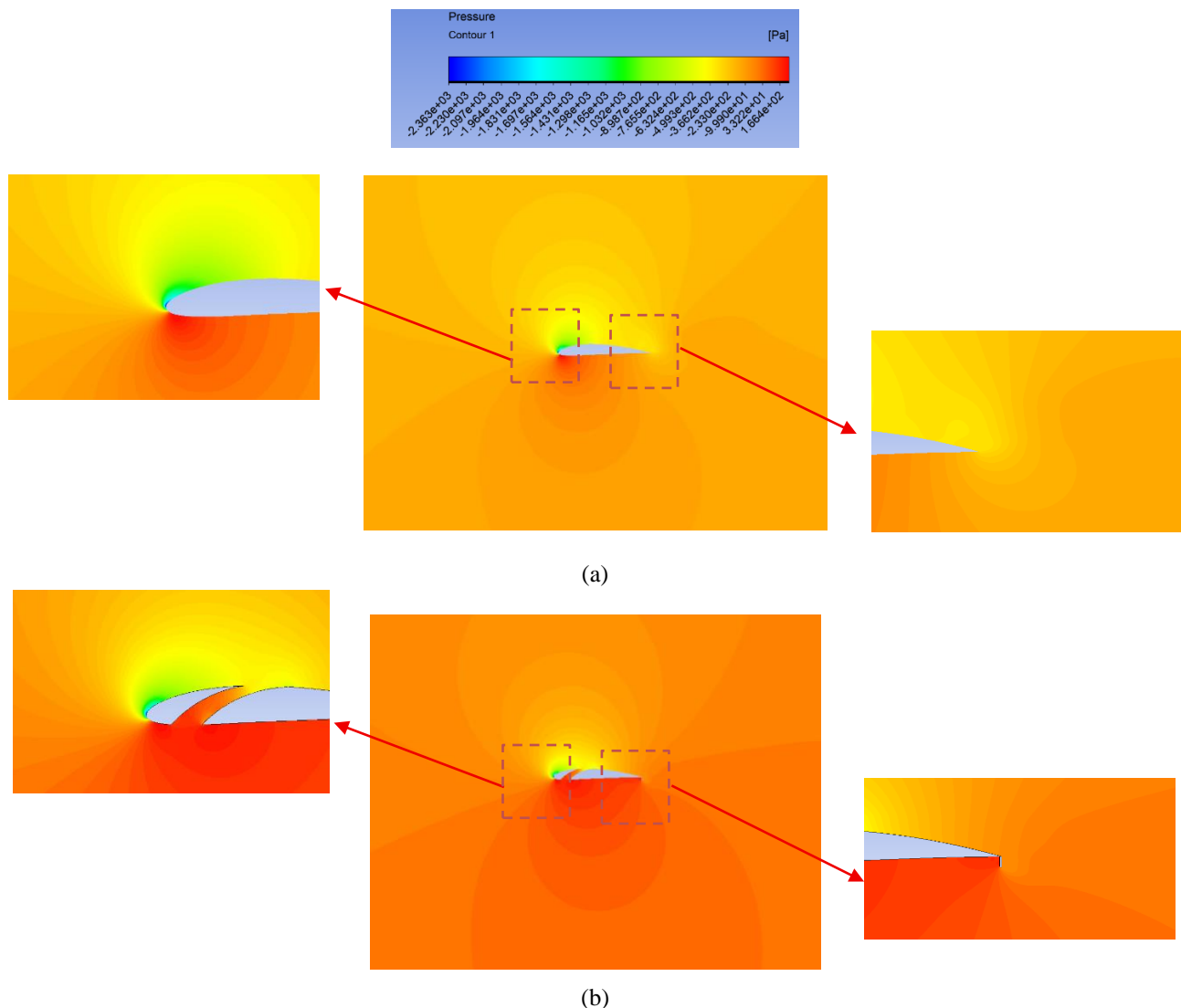


**Figure 7.** Pressure contour, (a) Pressure original (b) Pressure optimization

In **Figure 8** on the other hand, the flow characteristics are significantly improved for the optimized NACA 4412 airfoil, which features both an internal slot and a Gurney flap at the same angle of attack. The internal slot acts as a passive flow control device, helping to delay or prevent boundary layer separation by re-energizing the boundary layer with high-momentum fluid from the pressure side. Controlled vortex structures created by the Gurney flap downstream of the trailing edge increase circulation over the airfoil, augmenting virtual camber.

The implementation of this dual modification strategy has been demonstrated to yield several notable outcomes, including enhanced flow velocity distribution, more organized flow patterns, and a substantial delay in flow separation. The aerodynamic enhancements under consideration have been demonstrated to result in superior performance characteristics, particularly when operating at elevated angles of attack. It has been observed that conventional airfoils typically experience performance degradation under these conditions. This double-change plan has been shown to improve flow speed spread, increase order in the flow, and significantly delay flow breakaway. The shape changes being examined have been shown to provide better working features, primarily when used at high tilt angles. It is observed that regular wing shapes often fail to perform well under these conditions.

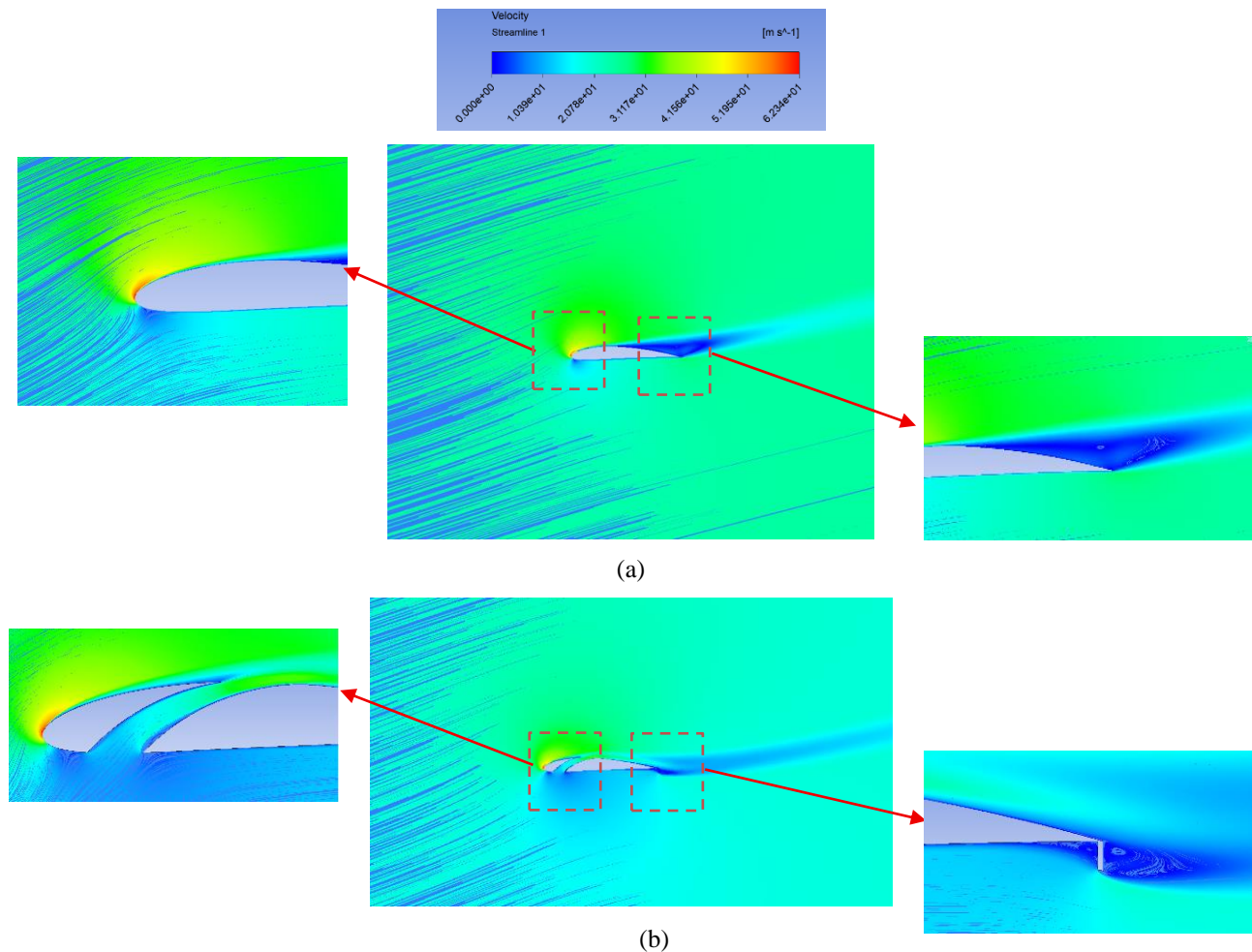


**Figure 8.** Velocity streamline, (a) Streamline original (b) Streamline Optimization

In **Figure 9** a detailed investigation of the baseline NACA 4412 airfoil's velocity field reveals conventional flow characteristics and indicates velocity gradients around the airframe structure. The pressure distribution on the lower surface is higher than that of the upper surface, resulting in considerable lift. Medium-sized turbulence is caused by flow separation in the upper back part of the airfoil. The characteristic features of conventional airfoils at higher angles of attack include the formation of the wake and boundary layer development in the velocity field. Turbulence mixing and moderate velocity deficits are observed in the wake region behind the trailing edge, indicating energy losses caused by flow separation and detachment of the boundary layer from the upper surface.

The modified configuration incorporating internal slot and Gurney flap substantially alters pressure distribution and velocity characteristics. Enhanced lower-surface pressure coupled with reduced upper-surface pressure improves flow attachment, resulting in delayed separation and increased flow stability. The internal slot energizes the boundary layer, producing streamlined velocity gradients and maintained flow coherence along the upper surface contour. This configuration achieves superior aerodynamic efficiency through reduced viscous losses, enhanced pressure differential, and decreased wake width. The optimized flow field demonstrates increased momentum retention and improved CL/CD ratio, validating the combined modification's effectiveness in enhancing NACA 4412 performance.

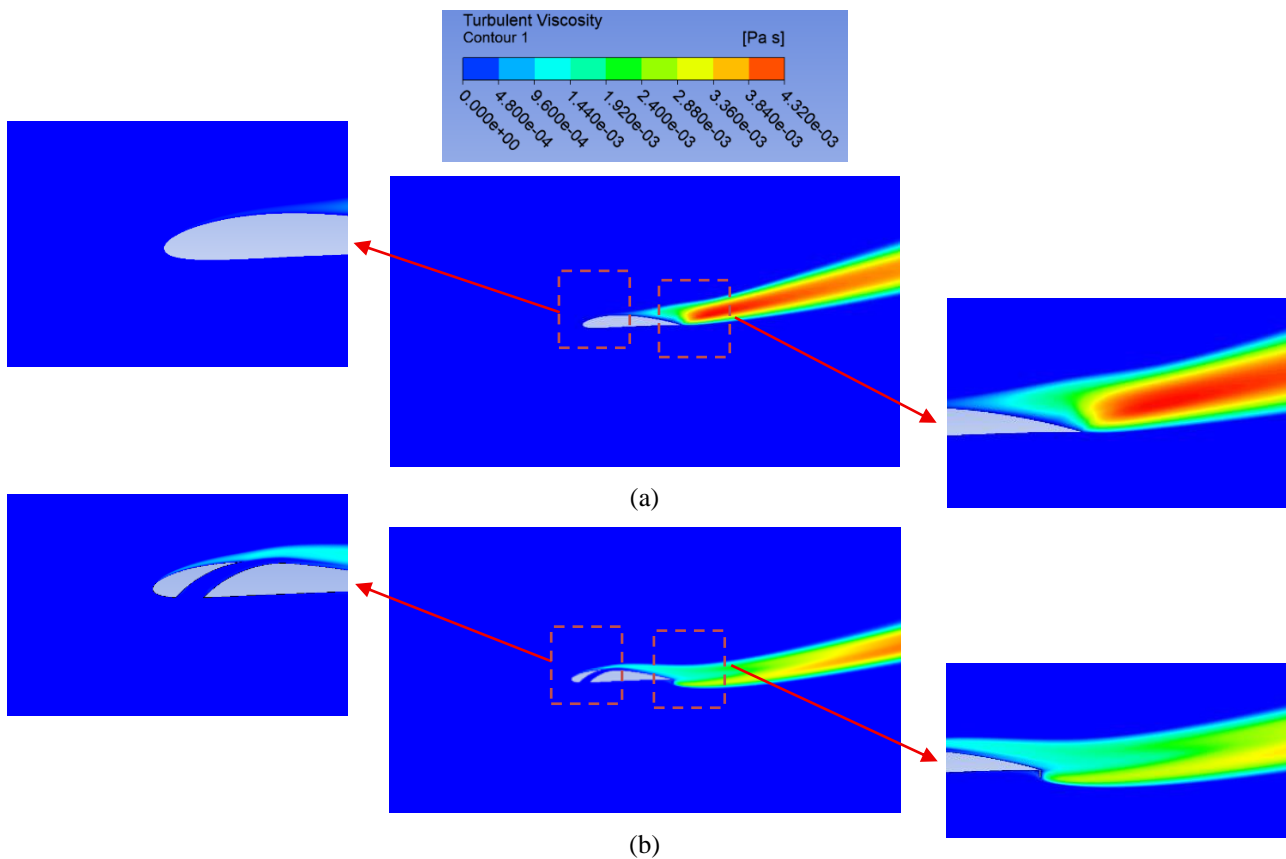


**Figure 9.** Turbulent, (a) Turbulent original (b) Turbulent Optimization

#### 4. Conclusion

This study successfully developed a more efficient NACA 4412 airfoil design by adding geometric modifications such as internal slot and gurney flap. CFD simulation methods and genetic algorithm optimization found that the lift coefficient of the optimized design could be increased by up to 75.68% compared to the initial design. Furthermore, the stall angle has been increased from  $14^\circ$  to  $16^\circ$ , and the overall aerodynamic efficiency has been enhanced. Pressure distribution and flow patterns also indicate that this improvement can stabilize the flow and delay the occurrence of separation. These findings suggest that combining internal slot with gurney flap effectively improves airfoil aerodynamic performance, particularly in situations requiring high lift at steep angles of attack. Similar approaches can be applied to other airfoils in the future to develop more adaptable and efficient aerodynamic designs.

#### Acknowledgement

The authors would like to express their gratitude to the Department of Mechanical Engineering, Faculty of Engineering, Semarang State University, for providing access to laboratories and institutional support that facilitated this research.

## References

- [1] Rayhan AM, Hossain MS, Mim RH, et al. Computational and experimental study on the aerodynamic performance of NACA 4412 airfoil with slot and groove. *Heliyon*; 10. Epub ahead of print 15 June 2024. DOI: 10.1016/j.heliyon.2024.e31595.
- [2] saxena G, agrawal M. Aerodynamic analysis of NACA 4412 airfoil using CFD. *Int J Emerg Trends Eng Dev Issue*; 3.
- [3] Ni Z, Dhanak M, Su T chow. Improved performance of a slotted blade using a novel slot design. *J Wind Eng Ind Aerodyn* 2019; 189: 34–44.
- [4] Chandra S, Tyagi R. Study of Eppler 423 Airfoil with Gurney Flap and Vortex Generators. *Adv Aerosp Sci Technol* 2020; 05: 1–19.
- [5] Bahatmaka A, Kim DJ, Chrismianto D, et al. Optimization of thrust propeller design for an ROV (Remotely Operated Vehicle) consideration by Genetic Algorithms. *MATEC Web Conf*; 138. Epub ahead of print 2017. DOI: 10.1051/mateconf/201713807003.
- [6] Bahatmaka A, Kim DJ, Anis S. A Validation Simulation using OpenFOAM: Nozzle Length and Angle Effect on the Ducted Propeller Performance. *IOP Conf Ser Earth Environ Sci*; 1083. Epub ahead of print 2022. DOI: 10.1088/1755-1315/1083/1/012088.
- [7] Aftab SMA, Ahmad KA. CFD study on NACA 4415 airfoil implementing spherical and sinusoidal Tubercle Leading Edge. *PLoS One* 2017; 12: 1–27.
- [8] Anil Kumar B, Manjunath S, Ganganna R. Computational Investigation of Flow Separation in Incompressible Aerodynamic Regime. *Int J Innov Res Sci Eng Technol (An ISO 2007)*; 3297: 470–476.
- [9] Karthikeyan K V., Harish R. Enhanced aerodynamic performance of NACA4412 airfoil through integrated plasma actuator and Gurney flap flow control. *Results Eng*; 25. Epub ahead of print 2025. DOI: 10.1016/j.rineng.2025.103977.
- [10] Bode F, Joldos T, Sirbu GM, et al. Impact of realistic boundary conditions on CFD simulations: A case study of vehicle ventilation. *Build Environ* 2025; 267: 112264.
- [11] Lu S, Liu J, Hekkenberg R. Mesh properties for rans simulations of airfoil-shaped profiles: A case study of rudder hydrodynamics. *J Mar Sci Eng*; 9. Epub ahead of print 2021. DOI: 10.3390/jmse9101062.
- [12] Akram MT, Kim MH. CFD analysis and shape optimization of airfoils using class shape transformation and genetic algorithm—part i. *Appl Sci*; 11. Epub ahead of print 2021. DOI: 10.3390/app11093791.
- [13] Suprayitno, Yu JC, Aminuddin, et al. Airfoil aerodynamics optimization under uncertain operating conditions. *J Phys Conf Ser*; 1446. Epub ahead of print 2020. DOI: 10.1088/1742-6596/1446/1/012014.
- [14] Julian J, Iskandar W, Wahyuni F. Aerodynamics Improvement of NACA 0015 by Using Co-Flow Jet. *Int J Mar Eng Innov Res*; 7. Epub ahead of print 2022. DOI: 10.12962/j25481479.v7i4.14898.
- [15] Wang Y, Shimada K, Barati Farimani A. Airfoil GAN: encoding and synthesizing airfoils for aerodynamic shape optimization. *J Comput Des Eng* 2023; 10: 1350–1362.
- [16] Popov AV, Botez RM, Labib M. Transition point detection from the surface pressure distribution for controller design. *J Aircr* 2008; 45: 23–28.
- [17] Hassan A. Predicted Aerodynamic Characteristics of a NACA 0015 Airfoil Having a 25% Integral-type Trailing Edge Flap. *Nasa Tech Pap*; CR-1999-20.
- [18] *Goldberg\_Genetic\_Algorithms\_in\_Search.pdf*. Canada: Addison-Wesley Publishing Company, Inc.
- [19] Tyagi A, Singh P, Rao A, et al. A novel framework for optimizing Gurney flaps using RBF surrogate model and cuckoo search algorithm. *Acta Mech* 2024; 235: 3385–3404.
- [20] Lee M, Park G, Park C, et al. Improvement of Grid Independence Test for Computational Fluid Dynamics Model of Building Based on Grid Resolution. *Adv Civ Eng*; 2020. Epub ahead of print 2020. DOI: 10.1155/2020/8827936.
- [21] NASA. Bernoulli ' s Principle principles of flight. *Museum BOX* 2010; 38 pages.